RESEARCH PAPER

Arvelexin from *Brassica rapa* suppresses NF-κB-regulated pro-inflammatory gene expression by inhibiting activation of IκB kinase

Ji-Sun Shin[1,3], Young-Su Noh[1,3], Yong Sup Lee[2], Young-Wuk Cho[3], Nam-In Baek[4], Myung-Sook Choi[5], Tae-Sook Jeong[6], Eunkyung Kang[7], Hae-Gon Chung[7] and Kyung-Tae Lee[1,2,3]

Departments of [1]*Pharmaceutical Biochemistry* and [2]*Life and Nanopharmaceutical Science, College of Pharmacy, Kyung Hee University, Seoul, Korea,* [3]*Department of Biomedical Science, College of Medical Science, Kyung Hee University, Seoul, Korea,* [4]*Graduate School of Biotechnology and Plant Metabolism Research Center, Kyung Hee University, Suwon, Korea,* [5]*Department of Food Science and Nutrition, Kyungpook National University, Daegu, Korea,* [6]*National Research Laboratory of Lipid Metabolism and Atherosclerosis, Korea Research Institute of Bioscience and Biotechnology, Daejeon, Korea, and* [7]*GangHwa Agricultural R&D Center, Incheon, Korea*

BACKGROUND AND PURPOSE

Brassica rapa species constitute one of the major sources of food. In the present study, we investigated the anti-inflammatory effects and the underlying molecular mechanism of arvelexin, isolated from *B. rapa*, on lipopolysaccharide (LPS)-stimulated RAW264.7 macrophages and on a model of septic shock induced by LPS.

EXPERIMENTAL APPROACH

The expression of Inducible nitric oxide synthase (iNOS) and COX-2, TNF-α, IL-6 and IL-1β were determined by Western blot and/or RT-PCR respectively. To elucidate the underlying mechanism(s), activation of NF-κB activation and its pathways were investigated by electrophoretic mobility shift assay, reporter gene and Western blot assays. In addition, the *in vivo* anti-inflammatory effects of arvelexin were evaluated in endotoxaemia induced with LPS.

KEY RESULTS

Promoter assays for iNOS and COX-2 revealed that arvelexin inhibited LPS-induced NO and prostaglandin E_2 production through the suppression of iNOS and COX-2 at the level of gene transcription. In addition, arvelexin inhibited NF-κB-dependent inflammatory responses by modulating a series of intracellular events of IκB kinase (IKK)-inhibitor κBα (IκBα)-NF-κB signalling. Moreover, arvelexin inhibited IKKβ-elicited NF-κB activation as well as iNOS and COX-2 expression. Serum levels of NO and inflammatory cytokines and mortality in mice challenged injected with LPS were significantly reduced by arvelexin.

CONCLUSION AND IMPLICATIONS

Arvelexin down-regulated inflammatory iNOS, COX-2, TNF-α, IL-6 and IL-1β gene expression in macrophages interfering with the activation of IKKβ and p38 mitogen-activated protein kinase, and thus, preventing NF-κB activation.

Abbreviations

IκBα, inhibitor of NF-κB-α; IKKs, IκB kinases; iNOS, inducible nitric oxide synthase; LPS, lipopolysaccharide; MAPK, mitogen-activated protein kinase; PBS, phosphate-buffered saline; PGE$_2$, prostaglandin E$_2$

Introduction

Inflammation is a component of many human diseases, including arteriosclerosis, inflammatory bowel disease, arthritis, infectious diseases and cancer (Yamamoto and Gaynor, 2004). The pathogenesis of inflammation is a complex process, regulated by cytokine networks and the inductions of many pro-inflammatory genes, such as inducible nitric oxide synthase (iNOS), COX-2, TNF-α, IL-6 and IL-1β. Thus, the inhibition of pro-inflammatory mediator production presents a possible critical target for the screening of anti-inflammatory agents (Guzik et al., 2003). Inflammation is triggered by various pathogens and by tissue damage via receptor signals that stimulate the transcription factor NF-κB, mitogen-activated protein kinases (MAPKs) and interferon response factors. In particular, NF-κB is known to play an important role in the regulation of immune and inflammatory responses (Zhang and Ghosh, 2001). Under normal conditions, NF-κB dimers are present in the cytoplasm complexed with its inhibitor IκB (NF-κB-IκB complex). Activation leads to phosphorylation of IκB proteins and their subsequent recognition by ubiquitinating enzymes. The resulting proteasomal degradation of IκB proteins leads to translocation of NF-κB to the nucleus, where it binds to its consensus DNA binding sites to regulate the transcription of a large number of genes, which include pro-inflammatory cytokines, adhesion molecules, chemokines and inducible enzymes (Karin and Ben-Neriah, 2000). The IκB kinases (IKK complex) mediate phosphorylation of IκB proteins and represents a convergence point for most signal transduction pathways leading to NF-κB activation (Hacker and Karin, 2006). Accordingly, agents that modulate the IKK-IκB-NF-κB activation process could be potential treatments for inflammatory diseases (De Bosscher et al., 2000; Yamamoto and Gaynor, 2001).

Plants from the Brassicaceae family have been recognized as an important source of foods and account for a substantial portion of worldwide vegetable production. Among them, the group of *Brassica rapa* includes many important crops, such as the Chinese cabbage and the turnip, and in South Korea, turnips are cultivated commercially in GangHwa County, Kyunggi Province and are used to make Kimchi (Jung et al., 2008). Moreover, in traditional medicine, *B. rapa* is used to treat a variety of diseases, such as hepatitis, jaundice, furuncle and sore throats. Although *B. rapa* contains numerous biologically active compounds, such as flavonoids (isorhamnetin, kaempferol and quercetin glycosides) (Romani et al., 2006), phenylpropanoid derivatives (Romani et al., 2006), indole alkaloids (Schonhof et al., 2004) and sterol glucosides (Schonhof et al., 2004), the molecular targets and the mechanisms underlying their biological activities of these constituents are poorly defined. It is also known that arvelexin, one of the phytoalexins secreted in Brassicaceae along with caulilexin and indole-3-acetonitrile compounds, exerts antifungal activity (Pedras et al., 2008). Several phytoalexins exert a variety of biological activities> Thus, resveratrol found in many plants including grapes and berries has potent anti-inflammatory, anticancer and cardioprotective activities *in vitro* and *in vivo* (Sadruddin and Arora, 2009). Therefore, as a part of our on-going screening project to evaluate the anti-inflammatory potential of natural compounds, we isolated arvelexin (Figure 1A) from *B. rapa* and investigated the anti-inflammatory effects of arvelexin on lipopolysaccharide (LPS)-stimulated RAW 264.7 macrophages and then in a LPS-induced septic shock model.

Methods

Isolation of indole compounds from the root of B. rapa

B. rapa L. emend. Metzg was obtained from the GangHwa Agricultural R&D Center (Incheon, Korea), and its identity was confirmed by one of the authors (Dr Hae-Gon Chung). A voucher specimen (number 05157) has been deposited at the Laboratory of Natural Product Chemistry, Kyung Hee University (Suwon, Korea). Five kilograms of the fresh root skin of *B. rapa* was immersed in 80% MeOH solution (10 L) and left for 24 h at room temperature with occasional stirring. The extract was filtered and the remainder was extracted twice more using the same method. The resulting filtrates were combined and concentrated under reduced pressure at 40°C to obtain the MeOH extract (102 g). The MeOH extract (100 g) was then suspended in water (1 L) and extracted with ethyl acetate (1L × 2). The ethyl acetate and aqueous layers were then concentrated under reduced pressure at 40°C to yield an ethyl acetate fraction (BRE, 7 g) and a H_2O fraction (BRW, 89 g). The ethyl acetate fraction (BRE, 7 g) was applied to the silica gel column chromatography, eluted with n-hexane-ethyl acetate (10:1 → 5:1 → 3:1→ 1:1) and CHCl$_3$-MeOH (10:1 → 7:1 → 5:1 → 3:1 → 2:1 → 1:1) to yield 23 fractions (BRE1-BRE23). The fraction BRE7 (515 mg) was subjected to chromatography on an octadecyl silica gel column (φ 5 × 22 cm, MeOH-H_2O = 3:1) to give purified indole compounds, caulilexin C [1, BRE-7–1, 38 mg, *Ve/Vt* 0.01–0.12 (elution volume/total volume); TLC (RP-18 F_{254s}) R_f = 0.75, MeOH-H_2O = 5:1] and indole-3-acetonitrile [2, BRE7-3, 15 mg, *Ve/Vt* 0.13–0.21; TLC (RP-18 F_{254s}) R_f = 0.55, MeOH-H_2O = 5:1]. The fraction BRE9 (268 mg) was further separated on a octadecyl silica gel column and MeOH-H_2O was used as an eluting solution to give a purified indole compound, arvelexin [3, BRE9-3, 21 mg, *Ve/Vt* 0.50–0.63, TLC (SiO$_2$ F_{254}) R_f = 0.42 in n-hexane-EtOAc (1:1) (RP-18 F_{254}) R_f = 0.62 in MeOH-H_2O (2:1)]. The chemical structures of compounds 1–3 (Fig 1A) were determined by comparing their physicochemical and spectroscopic data with reported values (Pedras et al., 2003; Kim et al., 2004). The compounds used for this study were examined by HPLC and were >97% pure. The Shimadzu LC-20A was used for HPLC analysis, equipped with a UV detector (268 nm) (Shimadzu, Tokyo, Japan). Chromatography was performed on a Waters C$_{18}$ column (5 μm, 250 × 4.6 mm) set at 30°C. Aliquots of 20 μL of each sample solution were injected and eluted according to the following program at a flow rate of 0.7 mL·min^{-1}: 45% MeOH → 70% MeOH from 0 to 10 min, 75% MeOH → 90% MeOH from 20 to 25 min, 90% MeOH to 40 min. The peak of arvelexin was appeared at 16.62 min. A typical HPLC chromatogram is shown in (Figure S1).

Cell culture and sample treatment

The RAW 264.7 macrophage cell line was obtained from the Korea Cell Line Bank (Seoul, Korea). These cells were grown at
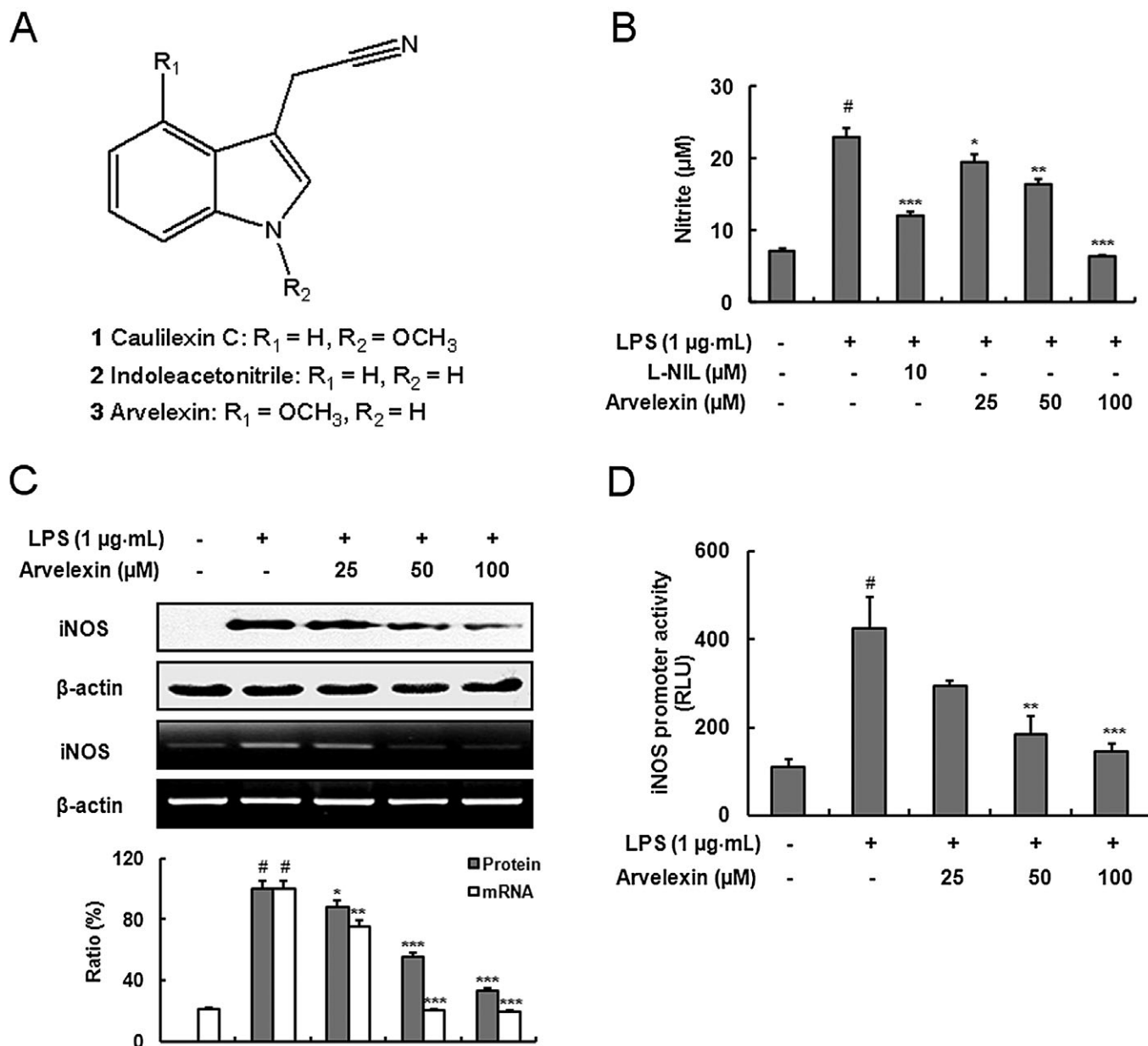
Figure 1

Chemical structures of indole compounds isolated from *B. rapa* and effects of arvelexin on the lipopolysaccharide (LPS)-induced NO production, iNOS expression and iNOS promoter activity in RAW 264.7 macrophages. (A) The chemical structures of arvelexin, caulilexin and indole-3-acetonitrile from the root skin of *B. rapa*. (B) Following pretreatment with arvelexin (25, 50, 100 μM) for 1 h, cells were treated with LPS (1 μg·mL^{-1}) for 24 h. Controls were not treated with LPS and arvelexin. L-NIL (10 μM) was used as a positive control. (C) Lysates were prepared from control, 24 h LPS (1 μg·mL^{-1}) alone or LPS plus with arvelexin (25, 50 or 100 μM). Total cellular proteins (30 μg) were resolved by SDS-PAGE, transferred to PVDF membranes and detected with specific antibodies. Total RNA was prepared for the RT-PCR analysis of iNOS from RAW 264.7 macrophages stimulated with LPS (1 μg·mL^{-1}) with/without arvelexin (25, 50 or 100 μM) for 4 h. The experiments were repeated three times and similar results were obtained. (D) Cells were transfected with a pGL3-iNOS promoter (−1592/+185) vector and the phRL-TK vector as an internal control. The level of luciferase activities was determined. Data are presented as the means ± SD of three independent experiments. #$P < 0.05$ versus the control group; *$P < 0.05$, **$P < 0.01$, ***$P < 0.001$ versus LPS-stimulated group.

37°C in Dulbecco's modified Eagle's medium (DMEM) supplemented with 10% fetal bovine serum, penicillin (100 units·mL^{-1}) and streptomycin sulphate (100 μg·mL^{-1}) in a humidified atmosphere of 5% CO$_2$. Cells were incubated with arvelexin at concentrations of 25, 50 and 100 μM, or with an appropriate control, and then stimulated with LPS 1 μg·mL^{-1} for the indicated time. Various concentrations of tested compounds dissolved in DMSO were added to the medium. The final concentration of DMSO did not exceed 0.05%.

Nitrite determination

RAW 264.7 cells were plated at 5×10^5 cells per well in 24 well-plates and then incubated with or without LPS ($1 \mu g \cdot mL^{-1}$) in the absence or presence of various concentrations (25, 50 or 100 μM) of arvelexin for 24 h. Nitrite levels in culture media were determined using the Griess reaction assay and presumed to reflect NO levels (Kim *et al.*, 2008).

PGE$_2$, TNF-α, IL-1β and IL-6 assay

RAW 264.7 cells were pretreated with arvelexin for 1 h and then stimulated with LPS ($1 \mu g \cdot mL^{-1}$) for 24 h. Levels of PGE$_2$, TNF-α, IL-1β and IL-6 in the culture media were quantified using enzyme immunoassay (EIA) kits (R&D Systems, Minneapolis, MN, USA).

Western blot analysis

RAW 264.7 cells were collected by centrifugation and washed once with phosphate-buffered saline (PBS). The washed cell pellets were resuspended in extraction lysis buffer (50 mM HEPES pH 7.0, 250 mM NaCl, 5 mM EDTA, 0.1% Nonidet P-40, 1 mM phenylmethyl sulphonyl fluoride (PMSF), 0.5 mM dithiothreitol (DTT), 5 mM NaF and 0.5 mM Na orthovanadate) containing $5 \mu g \cdot mL^{-1}$ each of leupeptin and aprotinin and incubated with 20 min at 4°C. Cell debris was removed by microcentrifugation, followed by rapid freezing of the supernatants. The protein concentration was determined using the Bio-Rad protein assay reagent according to the manufacturer's instructions. Thirty micrograms of cellular protein from treated and untreated cell extracts was electroblotted onto a PVDF membrane following separation on a 10–12% SDS-PAGE. The immunoblot was incubated overnight with blocking solution (5% skim milk) at 4°C, followed by incubation for 4 h with a primary antibody. Blots were washed four times with Tween 20/Tris-buffered saline and incubated with a 1:1000 dilution of horseradish peroxidase-conjugated secondary antibody for 2 h at room temperature. Blots were again washed three times with Tween 20/Tris-buffered saline, and then developed by enhanced chemiluminescence (GE healthcare). Bio-Rad Quantity One® Software was used for the densitometric analysis.

RNA preparation and RT-PCR

Total cellular RNA was isolated by Easy Blue® kits (Intron Biotechnology, Seoul, Korea). From each sample, 1 μg of RNA was reverse-transcribed by MuLV reverse transcriptase, 1 mM deoxyribonucleotide triphosphate (dNTP) and oligo (dT$_{12–18}$) $0.5 \mu g \cdot \mu L^{-1}$. PCR analyses were performed on aliquots of the cDNA preparations to detect COX-2, iNOS, TNF-α, IL-1β, IL-6 and β-actin (as an internal standard) gene expression using a thermal cycler (Perkin Elmer Cetus, Foster City, CA, USA). Reactions were carried out in a volume of 25 μL containing; 1 unit of Taq DNA polymerase, 0.2 mM dNTP, ×10 reaction buffer and 100 pmol of 5′ and 3′ primers. After an initial denaturation for 2 min at 95°C, 26 or 30 amplification cycles were performed for iNOS (1 min of 95°C denaturation, 1 min of 60°C annealing and 1.5 min 72°C extension), COX-2 (1 min of 94°C, 1 min of 60°C and 1 min 72°C), TNF-α (1 min of 94°C, 1 min of 55°C and 1 min 72°C), IL-1β (1 min of 94°C, 1 min of 60°C and 1 min 72°C) and IL-6 (1 min of 94°C, 1 min of 56°C and 1 min 72°C). The PCR primers used in this study are listed below and were purchased from Bioneer (Seoul, Korea): sense strand iNOS, 5′-AAT GGC AAC ATC AGG TCG GCC ATC ACT-3′, anti-sense strand iNOS, 5′-GCT GTG TGT CAC AGA AGT CTC GAA CTC-3′; sense strand COX-2, 5′-GGA GAG ACT ATC AAG ATA GT-3′, anti-sense strand COX-2, 5′-ATG- GTC AGT AGA CTT TTA CA-3′; sense strand TNF-α, 5′-ATG AGC ACA GAA AGC-ATG ATC-3′, anti-sense strand TNF-α, 5′-TAC AGG CTT GTC ACT CGA ATT-3′; sense strand IL-1β, 5′-TGC AGA GTT CCC CAA CTG GTA CAT C-3′; anti-sense strand IL-1β, 5′-GTG CTG CCT AAT GTC CCC TTG AAT C-3′; sense strand IL-6, 5′-GAG GAT ACC ACT CCC AAC AGA CC-3′, anti-sense strand IL-6, 5′-AAG TGC-ATC ATC GTT GTT CAT ACA-3′; sense strand β-actin, 5′-TCA TGA AGT GTG ACG- TTG ACA TCC GT-3′, anti-sense strand β-actin, 5′-CCT AGA AGC ATT TGC GGT- GCA CGA TG-3′. After amplification, the PCR reactions were analysed by electrophoresis on 2% agarose gel and visualized by ethidium bromide staining and UV irradiation.

Nuclear extraction and electrophoretic mobility shift assay

RAW 264.7 macrophage cells were plated in 100 mm dishes (1×10^6 cells·mL^{-1}), and treated with arvelexin (25, 50 and 100 μM), stimulated with LPS for 1 h, washed once with PBS, scraped into 1 mL of cold PBS and pelleted by centrifugation. Nuclear extracts were prepared as described previously (Kim *et al.*, 2008). Cell pellets were resuspended in hypotonic buffer (10 mM HEPES, pH 7.9, 1.5 mM MgCl$_2$, 10 mM KCl, 0.2 mM PMSF, 0.5 mM DTT, $10 \mu g \cdot mL^{-1}$ aprotinin) and incubated on ice for 15 min. Cells were then lysed by adding 0.1% Nonidet P-40 and vortexed vigorously for 10 s. Nuclei were pelleted by centrifugation at $12\,000 \times g$ for 1 min at 4°C and resuspended in high salt buffer (20 mM HEPES, pH 7.9, 25% glycerol, 400 mM KCl, 1.5 mM MgCl$_2$, 0.2 mM EDTA, 0.5 mM DTT, 1 mM NaF, 1 mM sodium orthovanadate). Nuclear extracts (10 μg) were mixed with double-stranded NF-κB oligonucleotide. 5′-AGTTGAGGGGACTTTCCCAG GC-3′ end-labelled by [α-^{32}P] dCTP (underlying indicates a κB consensus sequence or a binding site for NF-κB/cRel homodimeric or heterodimeric complex) using DNA labelling system (Amersham Life Science). Binding reactions were performed at 37°C for 30 min in 30 μL of reaction buffer containing 10 mM Tris-HCl, pH 7.5, 100 mM NaCl, 1 mM EDTA, 4% glycerol, 1 μg of poly (dI-dC) and 1 mM DTT. The specificity of binding was examined by competition with the 80-fold unlabelled oligonucleotide. DNA–protein complexes were separated from the unbound DNA probe on native 5% polyacrylamide gels at 100 V in 0.5 × Tris-boric acid-EDTA (TBE) buffer. Gels were vacuum-dried for 1 h at 60°C and exposed to X-ray film at –70°C for 24 h.

Plasmid, transient transfection and luciferase assay

The mouse iNOS promoter plasmid (pGL3-iNOS; −1592/+185) and COX-2 promoter plasmid (pGL3-COX-2; −965/+39) were prepared as described previously (Lowenstein *et al.*, 1993; Kraemer *et al.*, 1996). Expression vectors encoding IKKβ-S177E/S181E (constitutively active form) were purchased from Addgene, Inc. RAW 264.7 cells were co-transfected with pGL3-COX-2, pGL3-iNOS or NF-κB-Luc

reporter plasmid with/without IKKβ encoding vector plus the phRL-TK plasmid (Promega, Madison, WI, USA) using Lipofectamine LTX™ (Invitrogen, CA, USA) as instructed by the manufacturers. After 4 h of transfection, cells were pretreated with arvelexin for 1 h and then stimulated with LPS (1 μg·mL⁻¹) for 18 h. Each well was washed with cold PBS and cells were lysed and the luciferase activity was determined using the Promega luciferase assay system (Promega, Madison, CA, USA). In another, RAW 264.7 cells were transfected with IKKβ-S177E/S181E vector using Lipofectamine LTX™ (Invitrogen, CA, USA). After 4 h of transfection, cells were treated with arvelexin for 24 h and then subjected to Western blot analysis.

Animals and treatment

All animal care and experimental procedures complied with University Guidelines and were approved by the Ethical Committee for Animal Care and the Use of laboratory animals, College of Pharmacy, Kyung Hee University (KHP-2010-10-3). Male C57BL/6 mice weighing 18–20 g were purchased from Orient Bio (Gyeonggi, Korea). Animals were housed 5–6 per cage at a constant temperature of 20 ± 5°C and fed standard laboratory chow under a 12 h dark/light cycle.

Septic shock in mice

Male C57BL/6 mice, 6–8 weeks old, were given arvelexin (50, 75 or 100 mg·kg⁻¹, p.o.). After 1 h, septic shock was induced by injecting LPS (*S. enterica*, 25 mg·kg⁻¹, i.p.). Test samples were first dissolved in 5% EtOH and 5% Cremophor and diluted with saline (vehicle). Survival rates were monitored over 84 h. To determine serum cytokine levels, samples were collected 12 h after LPS (25 mg·kg⁻¹, i.p.) induction. Cytokine levels were determined using mouse Bio-Plex pro™ assays (Bio-Rad, Hercules, CA, USA).

Statistical analysis

Results are expressed as the mean ± SD of triplicate experiments. Statistically significant values were compared using ANOVA and Dunnett's *post hoc* test, and P-values of less than 0.05 were considered statistically significant.

Materials

Dulbecco's modified Eagle's medium (DMEM), fetal bovine serum, penicillin and streptomycin were obtained from Life Technologies Inc. (Grand Island, NY, USA). COX-2, p65, p50, anti-phospho-IκBα, anti-phospho-IKKα/β, anti-phospho-extracellular signal related kinase (p-ERK), anti-phospho-p38, anti-phospho-JNK, IκB, IKKα, IKKβ, ERK, p38, JNK, poly(ADP ribose)polymerase (PARP), β-actin monoclonal antibodies and peroxidase-conjugated secondary antibody were purchased from Santa Cruz Biotechnology Inc. (Santa Cruz, CA, USA). The enzyme immunoassay (EIA) kits for prostaglandin E₂ (PGE₂), TNF-α, IL-1β and IL-6 were obtained from R&D Systems (Minneapolis, MN, USA). Random oligonucleotide primers and M-MLV reverse transcriptase were purchased from Promega (Madison, WI, USA). dNTP Mix and ex Taq were obtained from TaKaRa (Seoul, Korea). COX-2, TNF-α, IL-1β, IL-6 and β-actin oligonucleotide primers were purchased from Bioneer (Seoul, Korea). 3-(4,5-Dimethylthiazol-2-yl)-2,5-diphenyl tetrazolium bromide (MTT), sulphanilamide, aprotinin, leupeptin, PMSF, DTT, NS-398, L-N⁶-(1-iminoethyl) lysine (L- NIL), LPS (*Escherichia coli*, serotype 0111:B4), LPS (*Salmonella enterica*, serotype enteritidis), Triton X-100 and all other chemicals were purchased from Sigma Chemical Co. (St. Louis, MO, USA).

Results

Arvelexin inhibited LPS-induced NO production and iNOS expression in RAW 264.7 macrophages

Repeated column chromatography of the 80% methanol extract of the root skin of *B. rapa* resulted in the isolation of three indole acetonitriles, arvelexin, caulilexin C and indole-3-acetonitrile (Fig 1A). During the preliminary testing of the anti-inflammatory activities of these three compounds, arvelexin reduced the productions of NO and PGE₂ inflammatory mediators most in LPS-stimulated RAW 264.7 cells (Table 1). We therefore examined further the anti-inflammatory effects of arvelexin and the underlying mechanisms in macrophages. As shown in Figure 1B, arvelexin (25, 50 or 100 μM) inhibited LPS-induced NO production, dose-dependently, in RAW macrophages. L-NIL was used as an positive control for inhibition of NOS. Because LPS induces iNOS (Moncada *et al.*, 1991), the protein and mRNA expression of iNOS were determined. As shown in Figure 1C, arvelexin markedly inhibited LPS-induced iNOS protein and mRNA expression in the same manner as it inhibited NO production. Next, in order to confirm whether inhibition of iNOS expression levels by arvelexin was exerted at the transcriptional level, we analysed the transcriptional activity of the iNOS gene promoter, which contains a NF-κB site. As shown in Figure 1D, LPS significantly enhanced the iNOS promoter luciferase activity, and arvelexin inhibited this induction in a dose-dependent manner.

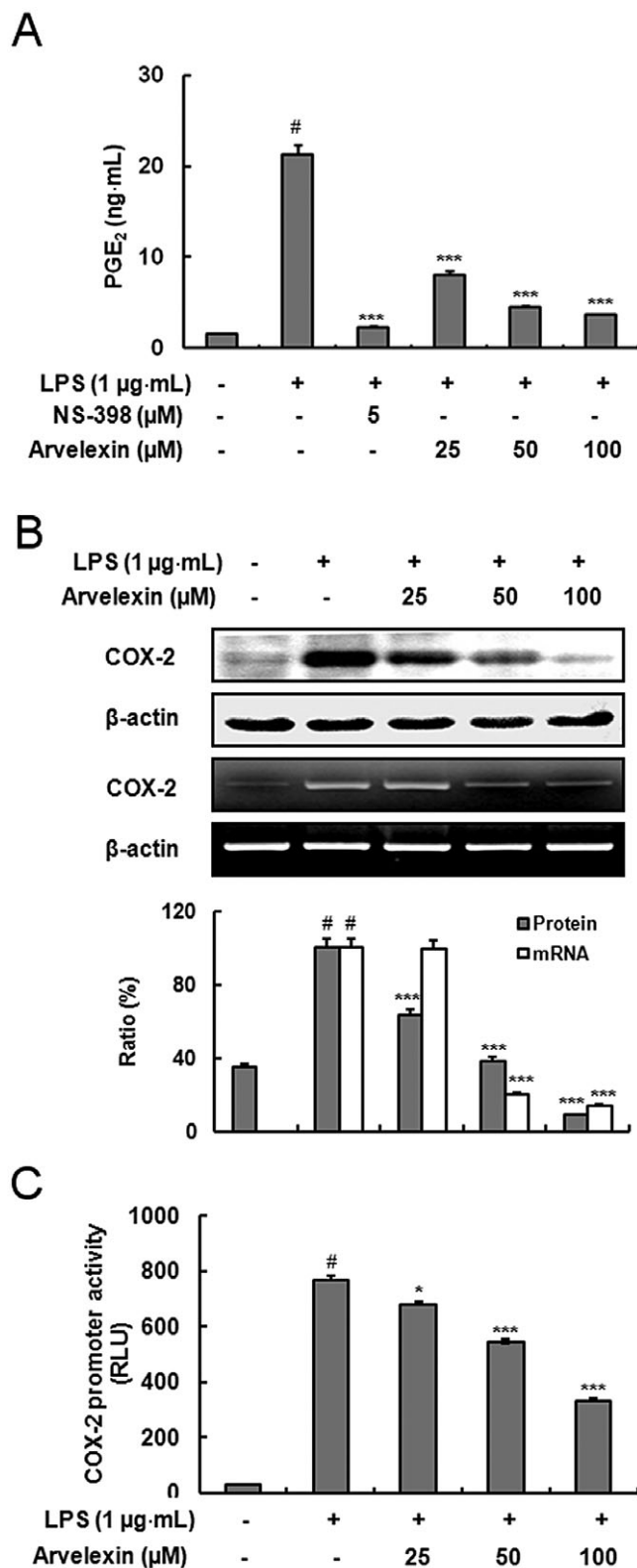## Arvelexin inhibited LPS-induced PGE₂ production and COX-2 expression in RAW 264.7 macrophages

To assess the effects of arvelexin on LPS-induced PGE₂ production in RAW 264.7 macrophage cells, PGE₂ was measured via enzyme immunoassay (EIA). Stimulation of cells with LPS (1 μg·mL⁻¹) resulted in a significant increase in PGE₂ produc-

Table 1

Effect of compounds isolated from *Brassica rapa* on cell viability, NO, and PGE₂ production in RAW 264.7 cells

Compound	IC₅₀ (μM) Cell viability	NO	PGE₂
Arvelexin	207	77	<25
Caulilexin	>400	>200	>200
Indole acetonitrile	145	164	131

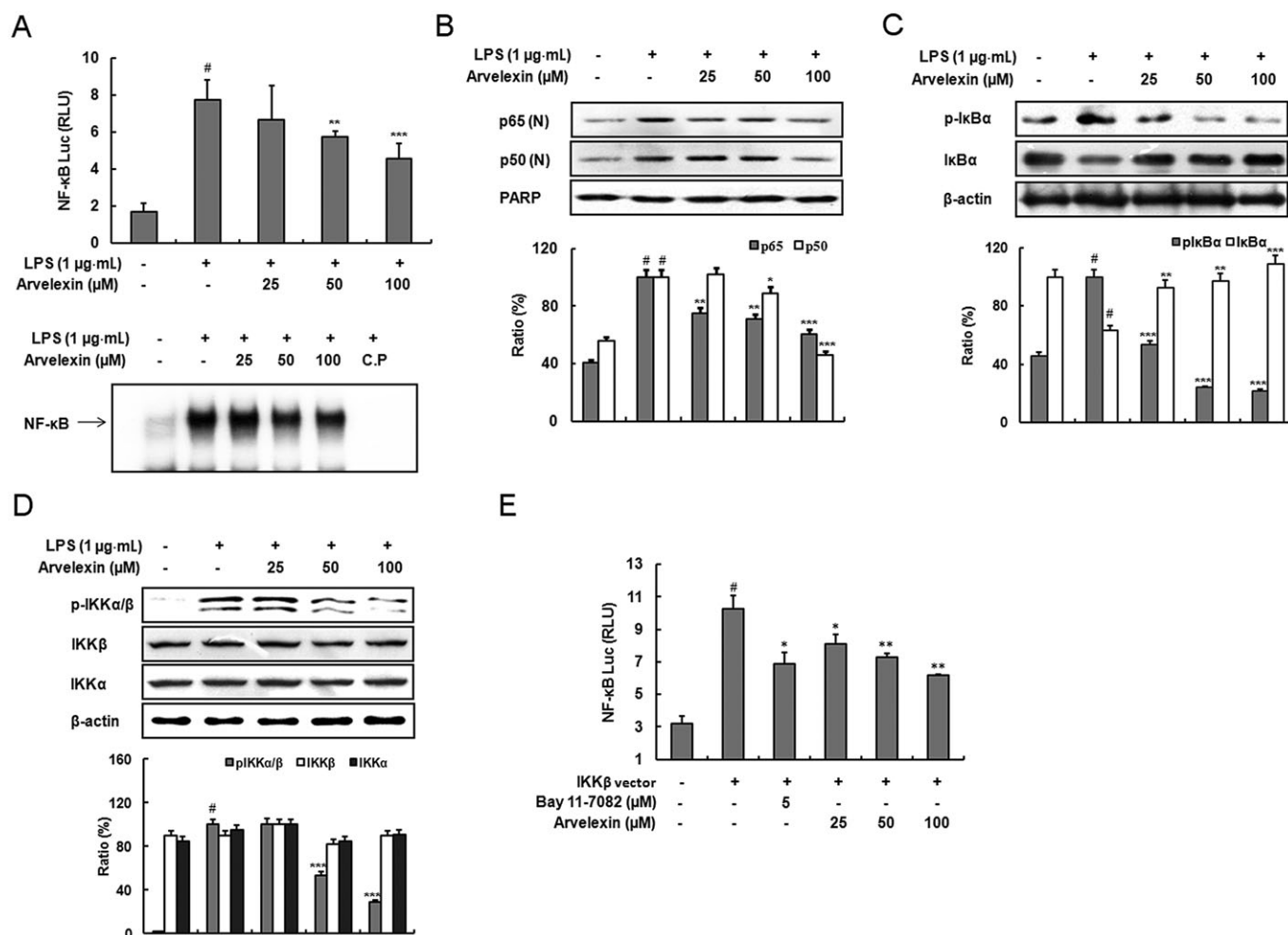IC₅₀ is defined as the concentration required for 50 % inhibition.

A

Figure 2

Effects of arvelexin on the LPS-induced PGE$_2$ production, COX-2 expression and COX-2 promoter activity in RAW 264.7 macrophages. (A) Following pretreatment with arvelexin (25, 50, 100 μM) for 1 h, cells were treated with LPS (1 μg·mL^{-1}) for 24 h. Controls were not treated with LPS and arvelexin. NS-398 (5 μM) was used as a positive control. (B) Lysates were prepared from control, 24 h LPS (1 μg·mL^{-1}) alone or LPS plus with arvelexin (25, 50 or 100 μM). Total cellular proteins (30 μg) were resolved by SDS-PAGE, transferred to PVDF membranes and detected with specific antibodies. Total RNA was prepared for the RT-PCR analysis of COX-2 from RAW 264.7 macrophages stimulated with LPS (1 μg·mL^{-1}) with/without arvelexin (25, 50 or 100 μM) for 4 h. The experiments were repeated three times and similar results were obtained. (C) Cells were transfected with a pGL3-COX-2 promoter (−965/+39) vector and the phRL-TK vector as an internal control. The level of luciferase activities was determined as described in *Methods*. Data are presented as the means ± SD of three independent experiments. #$P < 0.05$ versus the control group; *$P < 0.05$, **$P < 0.01$, ***$P < 0.001$ versus LPS-stimulated group.

B

C

arvelexin on protein and mRNA levels of COX-2. As shown in Figure 2B, COX-2 was markedly up-regulated by LPS at the protein and mRNA levels, and arvelexin strongly inhibited this up-regulation. Moreover, arvelexin inhibited LPS-induced COX-2 promoter luciferase activity in a dose-dependent manner (Figure 2C). These findings show that arvelexin transcriptionally down-regulates LPS-induced iNOS and COX-2 gene expression. In addition, MTT assays indicated that the suppressive effect of arvelexin on NO and PGE$_2$ production was not due to non-specific cytotoxicity (Table 1).

Arvelexin negatively regulates the NF-κB activation by inhibition of IKK complex activation

Accumulating data indicate that NF-κB is a major regulatory component of the inflammatory responses mediated by LPS or pro-inflammatory cytokines (Bonizzi and Karin, 2004). iNOS and COX-2 promoter regions contain NF-κB sites, which are necessary for inducing expression of these genes (Hacker and Karin, 2006). We therefore measured the effects of arvelxin on the transcriptional activity and DNA binding activities of NF-κB. Pretreatment with arvelexin reduced NF-κB-dependent luciferase activity and the DNA binding of NF-κB induced by LPS concentration dependently (Figure 3A). LPS markedly increased the translocation of p65 and p50 to the nucleus and arvelexin pretreatment significantly suppressed this nuclear translocation (Figure 3B). NF-κB remains inactive in the cytosol because of interaction with IκB. However, in response to inflammatory signals such as LPS, IκB is phosphorylated and subsequent degraded, resulting in activation and nuclear translocation of NF-κB (Karin and Ben-Neriah, 2000). Thus, we next examined whether arvelexin inhibited the phosphorylation and subsequent degradation of IκB. IκBα phosphorylation was increased after LPS treatment and arvelexin pretreatment significantly reduced this phosphorylation. In addition, LPS-induced IκBα degradation was significantly prevented by arvelexin (Figure 3C). These findings show that arvelexin

tion compared with unstimulated control cells (Figure 2A). Furthermore, pretreatment with arvelexin (25, 50 or 100 μM) markedly inhibited LPS-induced PGE$_2$ production. As a control for the inhibition of PGE$_2$ production, we used NS398 (5 μM) a COX-2 inhibitor. We also quantified the effects of
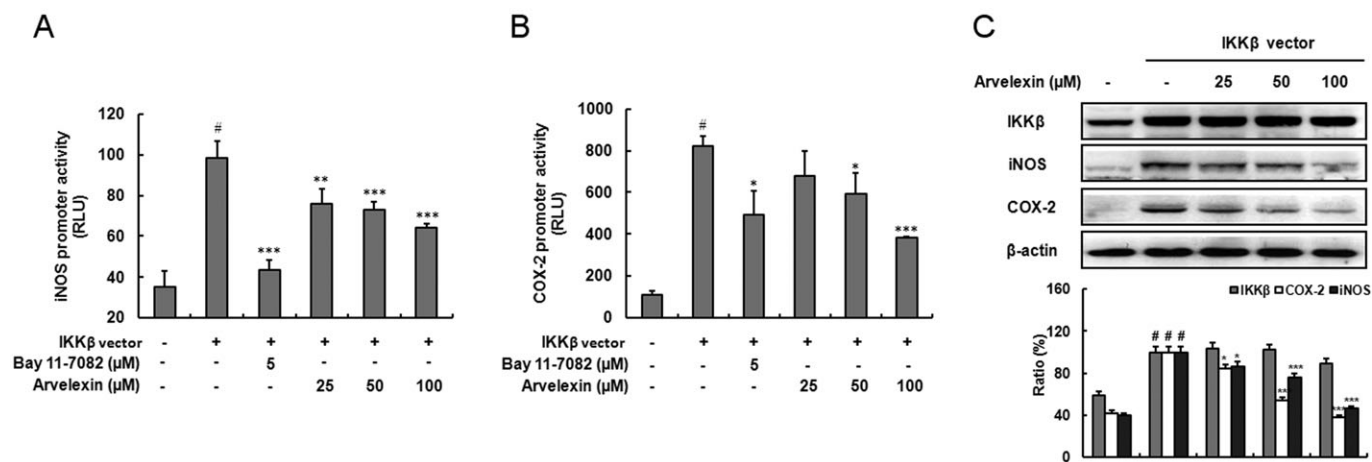
Figure 3

Effects of arvelexin on LPS-induced NF-κB activation. (A) Cells were transiently transfected with pNF-κB-luc reporter construct with the phRL-TK vector as an internal control. The level of luciferase activities was determined. Nuclear extracts from cells were prepared and used for analysis of NF-κB-DNA binding by electrophoretic mobility shift assay. The arrow indicates the position of the NF-κB band. Specificity of binding was examined by competition with 80-fold excess of unlabeled NF-κB oligonucleotide (cp). (B) Nuclear extracts were prepared for Western blot of p65 and p50 of NF-κB using specific anti-p65 and anti-p50 monoclonal antibodies. (C) Following pretreatment with arvelexin (25, 50 or 100 μM) for 1 h, cells were treated with LPS for 10 min. Total proteins were prepared and Western blot was performed using specific IκBα and pIκBα antibodies. (D) Following pretreatment with arvelexin (25, 50 or 100 μM) for 1 h, cells were treated with LPS (1 μg·mL⁻¹) for 5 min. Total cellular proteins (80 μg) were resolved by SDS-PAGE, transferred to PVDF membranes and detected with specific pIKKα/β, IKKα, IKKβ antibodies. (E) Cells were transiently transfected with pNF-κB-luc reporter construct and the phRL-TK vector as an internal control in combination with expression vector encoding IKKβ. The level of luciferase activities was determined. The data shown are representative of three independent experiments. Data are presented as the mean ± SD of three independent experiments. #$P < 0.05$ versus the control group; *$P < 0.05$, **$P < 0.01$, ***$P < 0.001$ versus LPS-stimulated or IKK-overexpressed group.

prevents NF-κB-DNA binding by inhibiting the phosphorylation and degradation of IκBα and the consequent nuclear translocation of p65/p50.

Inhibition of the phosphorylation of IκBα could be due to the direct inhibition of the corresponding IκB kinase (IKK). We therefore incubated purified IKKβ with various concentration of arvelexin before measuring its kinase activity *in vitro*. However, arvelexin did not affect catalytic activity of IKKβ *in vitro* (Figure S2). Next, we examined the effect of arvelexin on LPS-induced activation of IKKα/β, by Western blot using IKKα, IKKβ and phosphorylated IKKα/β antibodies.

As shown in Figure 3D, LPS strongly induced IKKα/β phosphorylation, whereas pretreatment with arvelexin (50 or 100 μM) significantly reduced this phosphorylation, without effects on total cellular IKKα and IKKβ. Furthermore, overexpression of IKKβ alone, without LPS, significantly induced NF-κB-dependent luciferase activity and pretreatment with arvelexin inhibited this IKKβ-induced NF-κB activation (Figure 3E). Collectively, our data demonstrated that arvelexin was able to inhibit LPS-induced NF-κB activation by preventing processes leading to the activation of the IKK complex.

Figure 4
Effects of arvelexin on IKKβ-elicited iNOS and COX-2 expression in RAW 264.7 macrophages. (A,B) Cells were transiently transfected with pGL3-iNOS promoter vector or pGL3-COX-2 promoter vector and the phRL-TK vector as an internal control in combination with expression vector encoding IKKβ. The level of luciferase activities were determined as described in Methods section. (C) Cells were transfected with expression vector encoding IKKβ. After 24 h of transfection, cells were treated with arvelexin for 24 h and then collected for Western Blot analysis. The data shown are representative of three independent experiments. Data are presented as the mean ± SD of three independent experiments. #$P < 0.05$ versus. the control group; *$P < 0.05$, **$P < 0.01$, ***$P < 0.001$ versus the IKK overexpressed group.

Arvelexin inhibited IKKβ-induced promoter activity and expression of iNOS and COX-2

As arvelexin down-regulated iNOS and COX-2 expression at the transcription level and inhibited IKKβ- and LPS-induced NF-κB activation, we examined the effect of arvelexin on IKKβ-induced iNOS and COX-2 promoter activities. As shown in Figure 4A and B, arvelexin significantly inhibited iNOS and COX-2 promoter activities induced by overexpressed IKKβ. Consistent with these results, treatment with arvelexin also inhibited IKKβ-induced iNOS and COX-2 protein expression (Figure 4C) as well as inhibiting LPS-induced expression (Figures 1C and 2B). These results suggest that arvelexin attenuated NF-κB-regulated expression of iNOS and COX-2 in activated macrophages.

Involvement of p38 and JNK MAPK pathway in arvelexin-induced anti-inflammatory responses

As the three MAPKs, ERK1/2, JNK and p38 MAPK, are known to be involved in NF-κB-regulated gene activation (Vermeulen *et al.*, 2003; Karin, 2005; Kefaloyianni *et al.*, 2006), we examined the effects of arvelexin on the LPS-induced phosphorylation of MAPKs in RAW 264.7 cells by Western blot. As shown in Figure 5A, arvelexin concentration-dependently suppressed the LPS-induced activation of p38 and JNK, but did not affect the phosphorylation of ERK1/2. Moreover, the specific inhibitors of p38 (SB203580) and JNK (SP600125), respectively, inhibited the iNOS and COX-2 promoter activities (Figure 5B). Consistent with these results, these inhibitors significantly attenuated the production of NO and PGE₂ (data not shown). Next, we determined whether p38 and JNK activation were involved in NF-κB activation by using reporter gene assays. Interestingly, the p38 inhibitor, but not the JNK inhibitor, significantly inhibited NF-κB activation

(Figure 5C). These results suggest that arvelexin can inhibit the signalling cascade involving both p38 MAPK-NF-κB and JNK, leading to suppression of iNOS and COX-2 expression in LPS-induced macrophages.

Arvelexin inhibited the LPS-induced production and mRNA expression of TNF-α, IL-6 and IL-1β

To evaluate the effect of arvelexin on other NF-κB-regulated pro-inflammatory cytokines, we further examined the production of TNF-α, IL-6, and IL-1β and their expression in LPS-stimulated macrophages pretreated with arvelexin. Pretreatment with arvelexin reduced LPS-induced TNF-α, IL-6, and IL-1β production and mRNA expression in a concentration-dependent manner (Figure 6A and B), showing that arvelexin suppresses the expression of these inflammatory genes. Collectively, arvelexin has the potential for inhibition not only iNOS and COX-2 expression but also a wide range of the pro-inflammatory genes, which are regulated by NF-κB.

Arvelexin inhibited the in vivo production of inflammatory mediators and protected mice from LPS-induced septic death

NF-κB-regulated pro-inflammatory mediators, such as NO and cytokines, play a pivotal role in the pathogenesis of sepsis (Opal, 2007). In view of the ability of arvelexin to attenuate the LPS-induced inflammatory mediators, we investigated the effects of arvelexin in an animal model of sepsis. LPS administration (25 mg·kg⁻¹, i.p.) markedly increased serum levels of NO, TNF-α, IL-6 and IL-1β, but pretreatment with arvelexin (50, 75 and 100 mg·kg⁻¹, p.o.) significantly decreased the production of these inflammatory mediators (Figure 7A). Subsequently, we observed that arvelexin improved survival during
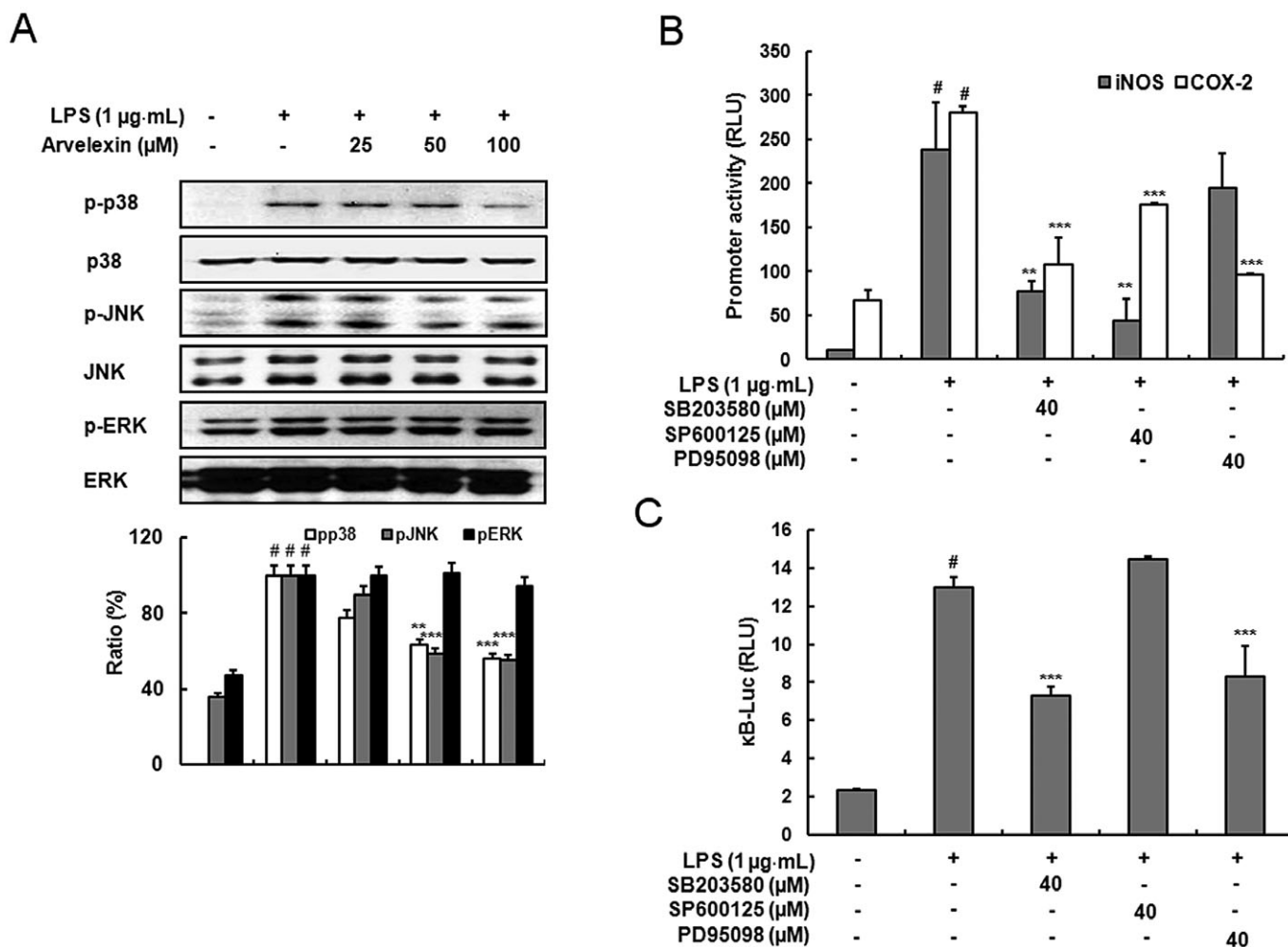
Figure 5

Involvement of MAPK with anti-inflammatory effect of arvelexin in RAW 264.7 macrophages. (A) Following pretreatment with arvelexin (25, 50 or 100 μM) for 1 h, cells were treated with LPS (1 μg·mL⁻¹) for 10 min. Whole cell lysates were analysed by Western blot using antibodies against activated MAPKs. (B) Cells were transiently transfected with pGL3-iNOS promoter vector or pGL3-COX-2 promoter vector and the phRL-TK vector as an internal control. After 4 h of transfection, cells were pretreated with SB203580 or SP600125 and then stimulated with LPS (1 μg·mL⁻¹) for 18 h. The level of luciferase activities was determined as described in *Methods*. (C) Cells were transiently transfected with pNF-κB-luc reporter construct and the phRL-TK vector as an internal control. After 4 h of transfection, cells were pretreated with SB203580, SP600125 or PD98059 and then stimulated with LPS (1 μg·mL⁻¹) for 18 h. The level of luciferase activities was determined. Data are presented as the mean ± SD of three independent experiments. #$P < 0.05$ versus the control group; *$P < 0.05$, **$P < 0.01$, ***$P < 0.001$ versus the LPS-stimulated group.

sepsis. As shown in Figure 7B, the injection of LPS resulted in 100% mortality at 36 h post injection in mice, but pretreatment with arvelexin reduced this to 30–70% at 84 h.
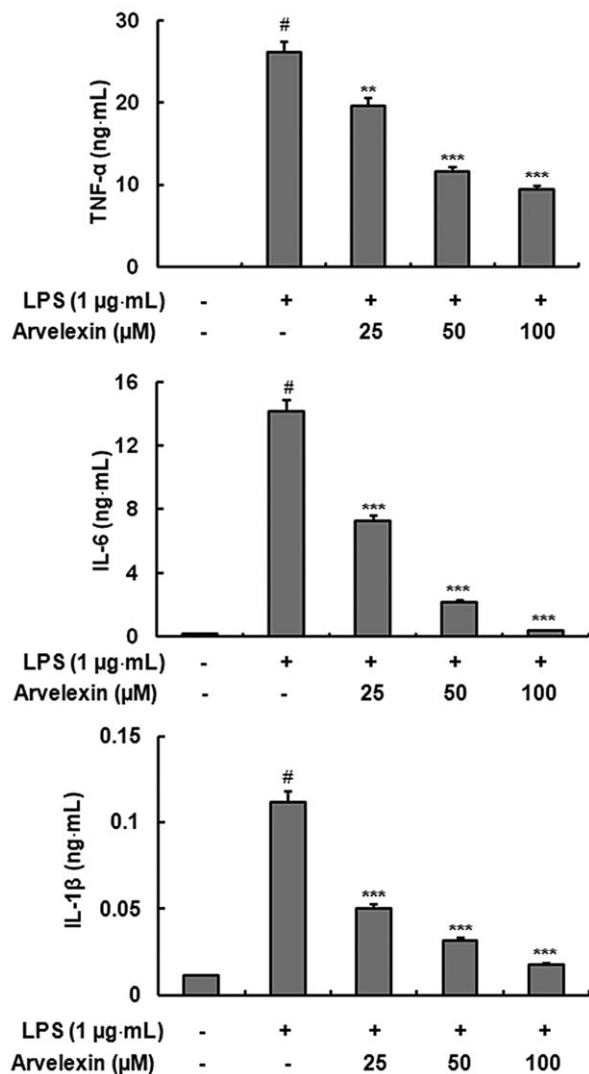
Discussion

In the present study, we demonstrated for the first time the anti-inflammatory activities of arvelexin isolated from *B. rapa*, both *in vitro* and *in vivo*, in LPS-stimulated RAW 264.7 macrophages and in an LPS-induced septic shock model. Furthermore, we showed that arvelexin inhibited inducible NF-κB activation and the subsequent induction of pro-inflammatory mediators, such as NO, PGE₂, TNF-α, IL-6 and IL-1β, and that it protected mice from lethal endotoxin shock.

The pathology of inflammation is initiated by complex processes triggered by microbial pathogens or their antigens, like LPS, a prototypic endotoxin (Corriveau and Danner, 1993). LPS can directly activate macrophages, which trigger the production of inflammatory mediators, such as PGE₂, NO, TNF-α, ILs and leukotrienes (Janeway and Medzhitov, 2002). In the present study, arvelexin clearly suppressed induction of iNOS and COX-2 through down-regulation of their promoter activities and subsequent production of NO and PGE₂ in LPS-stimulated macrophages.

Several lines of evidence indicate that NF-κB plays a critical role for the expression of iNOS, COX-2 and pro-inflammatory cytokines induced by inflammatory entities, such as LPS (Yamamoto and Gaynor, 2001). Accordingly, inhibition of NF-κB has shown to be effective at controlling inflammatory diseases in several animal models. For example,
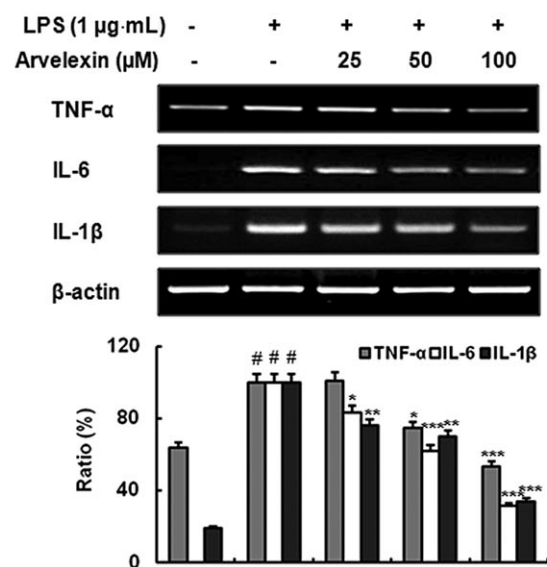
A

B

blocking NF-κB activity by the overexpression of IκBα has been reported to inhibit both inflammatory response and tissue destruction in rheumatoid synovium (Li and Verma, 2002). In a colitis model, inhibition of NF-κB by a IKK inhibitor ameliorated colonic inflammatory injury via down-regulation of pro-inflammatory cytokines (TNF-α, IL-1β and IL-6), mediated by NF-κB (Shibata *et al.*, 2007). Based on these reports, we tested whether arvelexin inhibited NF-κB activity in RAW 264.7 macrophage cells by using reporter gene assays and electrophoretic mobility shift assay. We found that arvelexin inhibited LPS-induced transcriptional activity and DNA binding of NF-κB in a dose-dependent manner in RAW macrophages.

Here, the anti-inflammatory effects of arvelexin have been also confirmed via investigation of several other inflammatory mediators in LPS-stimulated macrophages. The pro-inflammatory cytokines, such as TNF-α, IL-1β and IL-6, have profound effects on the regulation of immune reactions, haematopoiesis and inflammation (Mukaida, 2000). Arvelexin significantly inhibited LPS-induced TNF-α, IL-1β and IL-6 expression. Dysregulated production of cytokines plays a critical role in many inflammatory diseases and anti-cytokine strategies have proven to be clinically effective (McInnes and Schett, 2007). Several lines of evidence indicate that expression of pro-inflammatory cytokines, as well as iNOS and COX-2, is dependent on NF-κB in inflammatory environments (Yamamoto and Gaynor, 2001). By analogy with these results, we concluded that the inhibition of expression of pro-inflammatory mediators such as iNOS, COX-2 and cytokines, by arvelexin might result from suppression of NF-κB activation.

To identify the mechanisms involved in the inhibition of NF-κB activity by arvelexin, we tested the effect of arvelexin on NF-κB activation signals. NF-κB is composed mainly of two proteins: p65 and p50. In unstimulated cells, NF-κB exists in the cytosol in a quiescent form bound to its inhibitory protein, IκB (Karin and Ben-Neriah, 2000). Upon stimulation with LPS, IκB becomes phosphorylated and undergoes proteolytic degradation. Concomitantly, NF-κB becomes activated and translocates to the nucleus where it activates its target genes, such as those for iNOS, COX-2 and pro-inflammatory cytokines, by binding to its consensus sequence in their promoter regions (Surh *et al.*, 2001). In the
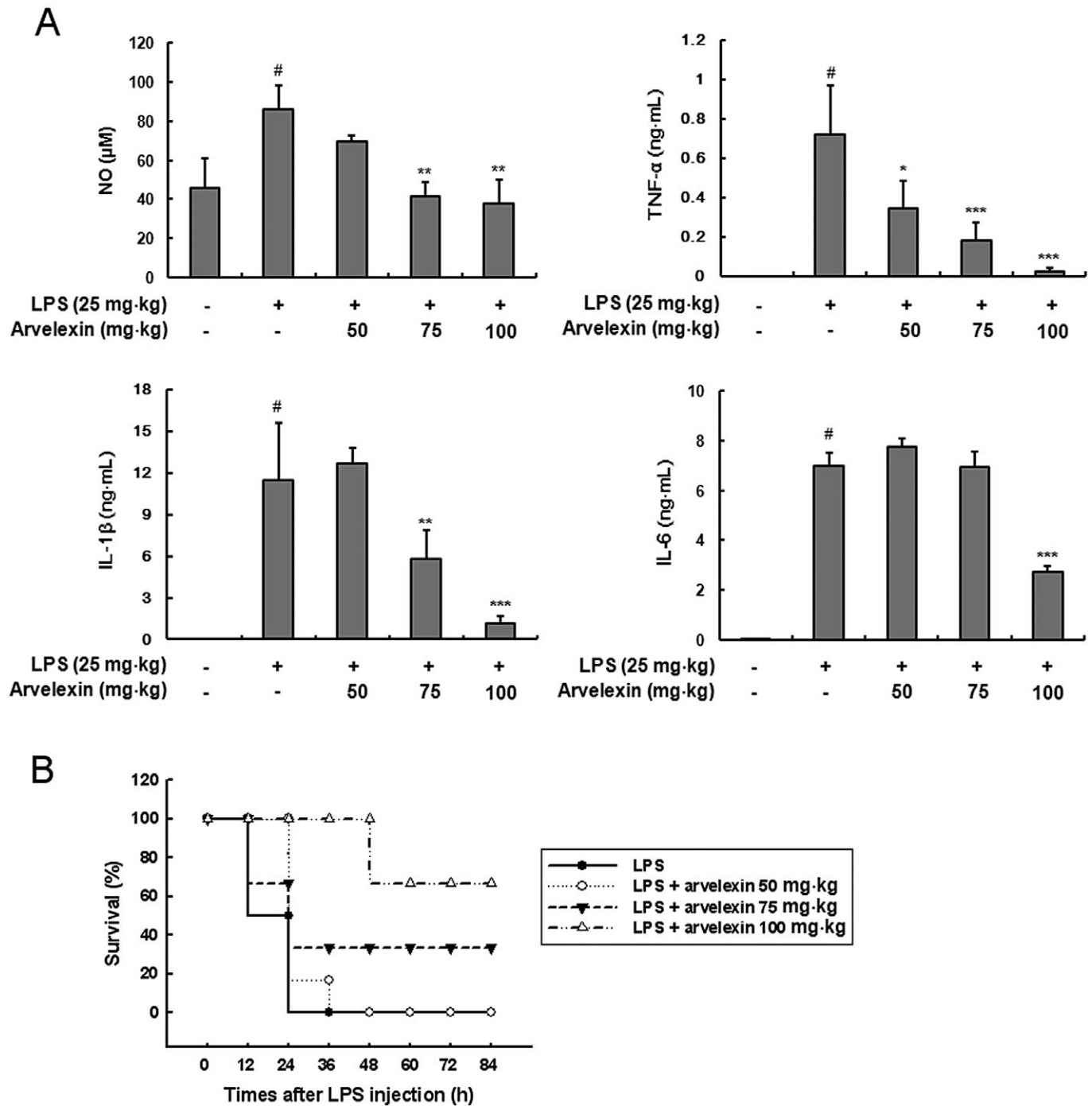
Figure 7

Effect of arvelexin on *in vivo* production of inflammatory mediators and lethality inLPS-induced septic shock model. (A) Arvelexin (50, 75 or 100 mg·kg^{-1}, p.o.) given to mice 1 h before LPS (25 mg·kg^{-1}, i.p.) injection. Serum was collected 12 h after LPS, the levels of NO and cytokines were determined by Griess reaction assay and Bio-Plex assays (*n* = 5–6). (B) Six mice per group were treated with vehicle only or arvelexin (50, 75 or 100 mg·kg^{-1}, p.o.) and after 1 h, LPS injected (25 mg·kg^{-1}, i.p.). Survival rates of these mice were observed over the next 84 h. *P < 0.05, **P < 0.01, ***P < 0.001 versus the LPS-injected group.

present study, Western blotting revealed that arvelexin inhibited LPS-induced IκBα phosphorylation and degradation and the subsequent nuclear translocations of p50 and p65 (NF-κB subunits), in a concentration-dependent manner.

We provided further evidence that inhibition of IκBα phosphorylation by arvelexin results from disturbance of IKK activation. IKK consists of two catalytic subunits, IKKα and IKKβ, and a regulatory subunit IKKγ/NEMO. It is suggested

that IKKα exhibits a catalytic activity of p65 phosphorylation (Ser536), whereas IKKβ is largely responsible for phosphorylation of both IκBα (at Ser32) and p65 (Perkins, 2007). As IKK is responsible for the first, critical step of NF-κB activation, this kinase may become a target for pharmacological intervention in a number of inflammatory conditions. Inhibition of IKK activity by arvelexin is not likely to result from direct interference with IKK catalytic activity, but is more likely to be mediated by reduction of phosphorylation-dependent activation, suggesting that the target for arvelexin is upstream of IKK. In previous studies, several plant-derived compounds suppress NF-κB-dependent gene expression by targeting the processes upstream of the IKK complex (Takada et al., 2005). To determine the effect of arvelexin on more proximal NF-κB-inducing signal pathway, we overexpressed IKKβ in cells. Our result showed that arvelexin inhibited IKK-elicited NF-κB transcriptional activity in a dose-dependent manner, suggesting that arvelexin suppresses NF-κB activation through down-regulation of IKK-mediated NF-κB pathway in LPS-stimulated RAW 264.7 cells.

In addition, available information showed that specific inhibitors of the ERK and p38 MAP kinase pathways block IKK/NF-κB activity and the transactivation activity of p65 (Vanden Berghe et al., 1998). To investigate whether the inhibition of NF-κB activation by arvelexin is mediated via the MAPK pathway, we investigated MAPK phosphorylation by Western blot in RAW 264.7 cells pretreated with arvelexin. Arvelexin suppressed the LPS-induced phosphorylation of p38 and JNK in a concentration-dependent manner. We also observed that pretreatment with the p38 inhibitor (SB203580) and the JNK inhibitor (SP600125) significantly reduced the iNOS and COX-2 promoter activity, which suggest that iNOS and COX-2 expression are regulated by p38 and JNK under our experimental conditions. In addition, we observed that SB203580 significantly decreased NF-κB transcriptional activation, whereas SP600125 did not show any effect on this activation. JNK can phosphorylate several transcription factors, such as c-Jun, JunB, c-fos, ATFs, and regulates the expression of several stress-responsive genes (Roy et al., 2008). Our results suggest that arvelexin may affect not only NF-κB but also other transcription factors. On the other hand, it has been previously demonstrated that p38 is necessary for NF-κB-dependent gene expression at the transcription level in macrophages (Carter et al., 1999). These results indicate that inhibition of p38 phosphorylation by arvelexin contributed to the inhibition of NF-κB activation in LPS-stimulated RAW264.7 cells.

Furthermore, several reports have demonstrated that suppression of p38 activity by the p38 inhibitor or siRNA significantly reduced IKK activity, indicating p38 may be associated with IKK-dependent NF-κB activation (Lee et al., 2009; Yoon et al., 2010). Our findings suggest that inhibition of pro-inflammatory mediators by arvelexin may be regulated by either both p38-IKK-NF-κB and JNK separately or together. Evidence to date suggests that TAK1 is a key regulator of the activations of IKKα/β, JNK and p38, but not of ERK (Adhikari et al., 2007); and therefore, arvelexin may target the molecules involved in the regulation of TLR4, IKKβ and TAK1.

In a recent study, we found that the ethanol extract of the roots of B. rapa (EBR) ameliorated cisplatin-induced nephro-toxicity in LLC-PK₁ cells by inducing anti-oxidant enzymes, such as glutathione peroxidase (Gpx), catalase and superoxide dismutase (SOD). Thus, we investigated whether arvelexin regulates cellular redox balance. We found that arvelexin induces the activation of NF-E2-related factor 2 (Nrf2), which plays an essential role in the regulation of redox balance and cytoprotective defences by inducing the expressions of cytoprotective and detoxification genes (Kong et al., 2010) (Figure S3A). Furthermore, arvelexin induced the expression of haem oxygenase 1 (HO-1, a Nrf2-regulated gene) in a time- and concentration-dependent manner (Figure S3B). To confirm the role of HO-1 in inflammatory response, we examined whether tin protoporphyrin IX (SnPP; a competitive inhibitor of HO-1) prevented the inhibitory effect of arvelexin on LPS-induced NO production and iNOS expression (Figure S3C and D). The results obtained indicated that the anti-inflammatory properties of arvelexin might be related to the inhibition of NF-κB activation and Nrf2-regulated HO-1 induction.

To confirm whether arvelexin also inhibits inflammatory responses in vivo, we evaluated the effects of arvelexin in a model of LPS-induced sepsis. Pretreatment with arvelexin reduced the serum levels of NO, TNF-α, IL-6 and IL-1β, and increased the survival rates of animals with established endotoxaemia induced by LPS. These results imply that the suppressive effects of arvelexin on NF-κB-regulated gene transcription in macrophages could result in an anti-inflammatory effect in an animal model of sepsis. Furthermore, we found that oral administration of arvelexin markedly inhibited the swelling of hind paws and MPO activity in a carrageenan-induced paw oedema model (a commonly used model for screening anti-inflammatory drugs) (Figure S4).

In summary, our results demonstrate that arvelexin exerted anti-inflammatory effects, which resulted from the inhibition of IKK-dependent NF-κB activation in macrophages, thereby inhibiting the expression of NF-κB-inducible iNOS, COX-2 and pro-inflammatory cytokines. More importantly, we demonstrated that arvelexin decreased the serum levels of these inflammatory mediators in vivo and protected mice from LPS-induced lethality. These findings on the anti-inflammatory action of arvelexin and its underlying mechanisms will enhance our understanding of the molecular pathology of inflammation.

Acknowledgements

Conflicts of interest

The authors have declared no conflicts of interest.

References

Adhikari A, Xu M, Chen ZJ (2007). Ubiquitin-mediated activation of TAK1 and IKK. Oncogene 26: 3214–3226.

Bonizzi G, Karin M (2004). The two NF-kappaB activation pathways and their role in innate and adaptive immunity. Trends Immunol 25: 280–288.

Carter AB, Knudtson KL, Monick MM, Hunninghake GW (1999). The p38 mitogen-activated protein kinase is required for NF-kappaB-dependent gene expression. The role of TATA-binding protein (TBP). J Biol Chem 274: 30858–30863.

Corriveau CC, Danner RL (1993). Antiendotoxin therapies for septic shock. Infect Agents Dis 2: 44–52.

De Bosscher K, Vanden Berghe W, Vermeulen L, Plaisance S, Boone E, Haegeman G (2000). Glucocorticoids repress NF-kappaB-driven genes by disturbing the interaction of p65 with the basal transcription machinery, irrespective of coactivator levels in the cell. Proc Natl Acad Sci USA 97: 3919–3924.

Ghosh S, Karin M (2002). Missing pieces in the NF-kappaB puzzle. Cell 109 (Suppl.): S81–S96.

Guzik TJ, Korbut R, Adamek-Guzik T (2003). Nitric oxide and superoxide in inflammation and immune regulation. J Physiol Pharmacol 54: 469–487.

Hacker H, Karin M (2006). Regulation and function of IKK and IKK-related kinases. Sci STKE 2006: re13.

Janeway CA Jr, Medzhitov R (2002). Innate immune recognition. Annu Rev Immunol 20: 197–216.

Jung UJ, Baek NI, Chung HG, Bang MH, Jeong TS, Lee KT et al. (2008). Effects of the ethanol extract of the roots of Brassica rapa on glucose and lipid metabolism in C57BL/KsJ-db/db mice. Clin Nutr 27: 158–167.

Karin M (2005). Inflammation-activated protein kinases as targets for drug development. Proc Am Thorac Soc 2: 386–390; discussion 394–395.

Karin M, Ben-Neriah Y (2000). Phosphorylation meets ubiquitination: the control of NF-[kappa]B activity. Annu Rev Immunol 18: 621–663.

Kefaloyianni E, Gaitanaki C, Beis I (2006). ERK1/2 and p38-MAPK signalling pathways, through MSK1, are involved in NF-kappaB transactivation during oxidative stress in skeletal myoblasts. Cell Signal 18: 2238–2251.

Kim SJ, Choi YH, Seo JH, Lee JW, Kim YS, Ryu SY et al. (2004). Chemical constituents from the root of Brassica campestris ssp rapa. Kor J pharmocon 35: 259–263.

Kim JY, Park SJ, Yun KJ, Cho YW, Park HJ, Lee KT (2008). Isoliquiritigenin isolated from the roots of Glycyrrhiza uralensis inhibits LPS-induced iNOS and COX-2 expression via the attenuation of NF-kappaB in RAW 264.7 macrophages. Eur J Pharmacol 584: 175–184.

Kong X, Thimmulappa R, Kombairaju P, Biswal S (2010). NADPH oxidase-dependent reactive oxygen species mediate amplified TLR4 signaling and sepsis-induced mortality in Nrf2-deficient mice. J Immunol 185: 569–577.

Kraemer SA, Arthur KA, Denison MS, Smith WL, DeWitt DL (1996). Regulation of prostaglandin endoperoxide H synthase-2 expression by 2,3,7,8,-tetrachlorodibenzo-p-dioxin. Arch Biochem Biophys 330: 319–328.

Lee JY, Kim H, Cha MY, Park HG, Kim YJ, Kim IY et al. (2009). Clostridium difficile toxin A promotes dendritic cell maturation and chemokine CXCL2 expression through p38, IKK, and the NF-kappaB signaling pathway. J Mol Med 87: 169–180.

Li Q, Verma IM (2002). NF-kappaB regulation in the immune system. Nat Rev Immunol 2: 725–734.

Lowenstein CJ, Alley EW, Raval P, Snowman AM, Snyder SH, Russell SW et al. (1993). Macrophage nitric oxide synthase gene: two upstream regions mediate induction by interferon gamma and lipopolysaccharide. Proc Natl Acad Sci USA 90: 9730–9734.

McInnes IB, Schett G (2007). Cytokines in the pathogenesis of rheumatoid arthritis. Nat Rev Immunol 7: 429–442.

Moncada S, Palmer RM, Higgs EA (1991). Nitric oxide: physiology, pathophysiology, and pharmacology. Pharmacol Rev 43: 109–142.

Mukaida N (2000). The roles of cytokine receptors in diseases. Rinsho Byori 48: 409–415.

Opal SM (2007). The host response to endotoxin, antilipopolysaccharide strategies, and the management of severe sepsis. Int J Med Microbiol 297: 365–377.

Pedras MS, Chumala PB, Suchy M (2003). Phytoalexins from Thlaspi arvense, a wild crucifer resistant to virulent Leptosphaeria maculans: structures, syntheses and antifungal activity. Phytochemistry 64: 949–956.

Pedras MS, Zheng QA, Gadagi RS, Rimmer SR (2008). Phytoalexins and polar metabolites from the oilseeds canola and rapeseed: differential metabolic responses to the biotroph Albugo candida and to abiotic stress. Phytochemistry 69: 894–910.

Perkins ND (2007). Integrating cell-signalling pathways with NF-kappaB and IKK function. Nat Rev Mol Cell Biol 8: 49–62.

Romani A, Vignolini P, Isolani L, Ieri F, Heimler D (2006). HPLC-DAD/MS characterization of flavonoids and hydroxycinnamic derivatives in turnip tops (Brassica rapa L. Subsp. sylvestris L.). J Agric Food Chem 54: 1342–1346.

Roy PK, Rashid F, Bragg J, Ibdah JA (2008). Role of the JNK signal transduction pathway in inflammatory bowel disease. World J Gastroenterol 14: 200–202.

Sadruddin S, Arora R (2009). Resveratrol: biologic and therapeutic implications. J Cardiometab Syndr 4: 102–106.

Schonhof I, Krumbein A, Bruckner B (2004). Genotypic effects on glucosinolates and sensory properties of broccoli and cauliflower. Nahrung 48: 25–33.

Shibata W, Maeda S, Hikiba Y, Yanai A, Ohmae T, Sakamoto K et al. (2007). Cutting edge: the IkappaB kinase (IKK) inhibitor, NEMO-binding domain peptide, blocks inflammatory injury in murine colitis. J Immunol 179: 2681–2685.

Surh YJ, Chun KS, Cha HH, Han SS, Keum YS, Park KK et al. (2001). Molecular mechanisms underlying chemopreventive activities of anti-inflammatory phytochemicals: down-regulation of COX-2 and iNOS through suppression of NF-kappa B activation. Mutat Res 480–481: 243–268.

Takada Y, Kobayashi Y, Aggarwal BB (2005). Evodiamine abolishes constitutive and inducible NF-kappaB activation by inhibiting IkappaBalpha kinase activation, thereby suppressing NF-kappaB-regulated antiapoptotic and metastatic gene expression, up-regulating apoptosis, and inhibiting invasion. J Biol Chem 280: 17203–17212.

Vanden Berghe W, Plaisance S, Boone E, De Bosscher K, Schmitz ML, Fiers W et al. (1998). p38 and extracellular signal-regulated kinase mitogen-activated protein kinase pathways

are required for nuclear factor-kappaB p65 transactivation mediated by tumor necrosis factor. J Biol Chem 273: 3285–3290.

Vermeulen L, De Wilde G, Van Damme P, Vanden Berghe W, Haegeman G (2003). Transcriptional activation of the NF-kappaB p65 subunit by mitogen- and stress-activated protein kinase-1 (MSK1). EMBO J 22: 1313–1324.

Yamamoto Y, Gaynor RB (2001). Therapeutic potential of inhibition of the NF-kappaB pathway in the treatment of inflammation and cancer. J Clin Invest 107: 135–142.

Yamamoto Y, Gaynor RB (2004). IkappaB kinases: key regulators of the NF-kappaB pathway. Trends Biochem Sci 29: 72–79.

Yoon YM, Lee JY, Yoo D, Sim YS, Kim YJ, Oh YK et al. (2010). Bacteroides fragilis enterotoxin induces human beta-defensin-2 expression in intestinal epithelial cells via a mitogen-activated protein kinase/I kappaB kinase/NF-kappaB-dependent pathway. Infect Immun 78: 2024–2033.

Zhang G, Ghosh S (2001). Toll-like receptor-mediated NF-kappaB activation: a phylogenetically conserved paradigm in innate immunity. J Clin Invest 107: 13–19.

Supporting information

Additional Supporting Information may be found in the online version of this article:

Figure S1 The purity of the isolated arvelexin from the root of B. rapa. (A) HPLC analysis of arvelexin. (B) Calculated amount of peaks. The compounds used for this study were examined by HPLC and were >97% pure.

Figure S2 Effects of arvelexin on IKKβ kinase activity. IKKβ kinase activity was measured using an HTScan IKKβ kinase assay kit. Purified IKKβ was incubated with various concentration of arvelexin (25, 50 or 100 µM) before the kinase reaction.

Figure S3 Induction of Nrf2/HO-1 by arvelexin involved with inhibition of NO production and iNOS protein expression in LPS-induced RAW 264.7 macrophages. (A) Nuclear extracts from cells were prepared and used for analysis of Nrf2-DNA binding by electrophoretic mobility shift assay. The arrow indicates the position of the Nrf2 band. Specificity of binding was examined by competition with 80-fold excess of unlabeled Nrf2 oligonucleotide. (B) At 0, 2, 4, 8, 12 h after the treatment of arvelexin, cells were collected for Western blot. And following treatment with arvelexin (25, 50 or 100 µM) for 8 h, cells were collected for Western blot. Total cellular proteins were resolving by SDS-PAGE, and detected with specific HO-1 antibody. (C, D) Cells were pretreated with SnPP (20 µM) for 30 min before the treatment of LPS (1 µg·mL^{-1}) in the present or absence of arvelexin and incubate for 24 h. Data are presented as the means ± SD of three independent experiments. $^{#}P < 0.05$ versus the control group; $^{***}P < 0.001$ versus LPS-stimulated group.

Figure S4 Inhibitory effects of arvelexin on carrageenan-induced paw oedema. (A) Arvelexin (25 mg·kg^{-1} or 100 mg·kg^{-1}, p.o.) was administered 1 h before carrageenan injection. Positive control animals were treated with ibuprofen (100 mg·kg^{-1}, p.o.). The paw volume was measured at 1, 3 and 5 h after carrageenan injection. (B) Soft tissues from carrageenan-injected paws were recovered at 5 h and homogenized. Amounts of MPO were determined using EIA kits. Values shown are the mean ± SD of three independent experiments ($n = 5–6$). $^{*}P < 0.05$, $^{**}P < 0.01$, $^{***}P < 0.001$ versus the carrageenan-injected group.